



Photo-Remediation, Antioxidant, Antibacterial And Antifungal Activity Of *Nyctanthes Arbor- Tristis* And *Terminalia Chebula* Silver Nanoparticles

Dr. Suchitra Naidu, Assistant Professor, Loyola academy, Hyderabad

Aishwariya Jena, Ciencia Life Sciences, Hyderabad

Dr. Y. Sabitha, Research Head, Ciencia Labs, Hyderabad

ABSTRACT

Since the beginning of recorded history, silver has been used to heal burns, ulcers, and various bacterial diseases in the way that involves metallic silver, silver nitrate, and silver sulfadiazine. However, utilization of these silver compounds has dramatically decreased as a result of the development of several medicines. In the present work, an effortless green synthesis approach for the production of stable silver nanoparticles using the halophyte plant *Nyctanthes arbor-tristis* and *Terminalia chebula* as the reducing/stabilizing agent was reported. The obtained silver nanoparticles (Ag NPs) were further characterized through UV-vis absorption spectroscopy, Scanning electron microscope (SEM), and Transmission electron microscope (TEM). Using UV-vis spectrophotometer the stability and also the formation of the Ag Np was tracked. Based on the growth kinetics of gram (+) *Bacillus*, gram (-) *E Coli*, and also *Aspergillus niger*. NPs from both the plants showed good antimicrobial activity with *T. chebula* showing the best result. None of the NPs from either of the plants showed antifungal activity. *T. chebula*-AgNP also showed good antioxidant activity compared to Nyc-AgNPs. In our study, we also found the NPs from both plants showing good photo-catalytic degradation of malachite green than methylene blue dye, with Nyc-AgNP showing the best result.

Keywords: AgNPs, *Nyctanthes arbor-tristis*, *Terminalia chebula*, Antimicrobial activity, Antioxidant assay, Photocatalytic degradation

1. INTRODUCTION

Since ancient times, silver has been employed as an antibacterial substance. Silver can now be created at the nanoscale thanks to recent developments in nanotechnology. The emergence of nanosilver materials in antimicrobial consumer goods and medical products, in addition to their potential electronic as well as transparent conductor applications, is fueling the growth of the nanosilver market, which is anticipated to increase in value from US\$290 million in 2011 to about US\$1.2 billion by 2016. Silver nanoparticles (AgNPs), which are included in a variety of nanosilver preparations, are composed of 20–15,000 silver atoms and typically have a diameter between 1 and 100 nm (Williams, 2008).

For a more environmentally friendly way to make nanoparticles, biological synthesis techniques have been used. Because of their slower kinetics and better control over crystal formation and stability, they have turned out to be superior approaches. The need for greater size and shape control for a wide range of nanotechnological applications has prompted an increase in research on synthesis methods. The utilization of ecologically friendly substances, such as plant extract, microorganisms, and have a number of advantages, including biocompatibility, non-toxicity, and is cost-effectiveness and have a number of advantages, including biocompatibility, non-toxicity, and cost-effectiveness method (Mohanpuria et al., 2008).

With the benefit of employing natural products and avoiding toxic reducing agents, organic solvents, and inefficient purifications with high cytotoxic residuals, efforts have recently been concentrated on creating new green chemical techniques of synthesizing AgNPs. These techniques substitute chemicals produced by living organisms like bacteria, fungus, or plants for the reducing and capping agents. For instance, chitosan made from several species of bacteria and dissolved in acetic acid is combined with AgNO₃. After that, gamma radiation is used to decrease the silver ions, and chitosan is used to stabilize them. Additionally, attempts have been made to create AgNPs in the lamellar space of montmorillonite/chitosan using the UV irradiation reduction approach without the need of reducing agents or heat treatment (Shameli et al., 2010). In addition, AgNPs have been created without the use of PVP by photo-reducing AgNO₃ in solutions of layered inorganic clay called laponite (Huang & Yang, 2008). These stabilizing chemicals prevent nanoparticles from clumping. Using these kinds of green synthesis has the drawback that there is a risk of contamination because of the dangerous bacteria that are produced during the purification process (Ge et al., 2014). As a result, owing to their antioxidant and antibacterial characteristics without utilizing harmful microbes, herbal extracts as well as essential oils are becoming more and more popular as green synthesis techniques (Vilas et al., 2014). However, employing plant extracts has the drawback of obtaining a wide range of particle sizes.

Due to their unique antimicrobial properties Ag NPs have been used in a lot of applications including clothing manufacturing, for preservation of food, for the purification of water (Zhang et al., 2014; Manjumeena et al., 2014). Most of the Ag NPs are being utilized in the medical sector because of their antibacterial, antifungal, antiviral and anti-inflammatory effects and also due to their property of enhancing wound healing.

These Ag NPs have been extensively used as an antibacterial cast in medical applications such as wound dressing, cardiovascular implants, in catheters, in orthopedic implants etc.

While many new prospective uses are actively being researched, the usage of Ag NPs in many commercial applications as well as certain therapeutic applications, such as wound dressings, is already well-established. Given their antimicrobial, and anti-inflammatory qualities, Ag NPs have a lot of potential, and recent study has also found unique osteoinductive capabilities. The biological processes and mechanisms behind these characteristics are not entirely known, yet. As Ag NP use continues to rise, it is necessary to do further research on, for instance, the relationship between the size and form of Ag NPs and their biological characteristics and toxicity. Before Ag NPs are widely used in medicine, it is imperative to thoroughly understand the processes underlying their effectiveness and toxicity. In the present work we report a green synthesis approach of silver nanoparticles using leaf extract of *Nyctanthes arbor-tristis* and *Terminalia chebula*.

2. MATERIALS AND METHODS

2.1 Selection and collection of plant material

Two different medicinal plants were selected for the synthesis of silver nanoparticles. Fresh and healthy leaves from *Terminalia chebula* (Haritaki), an Indian medicinal herb (Ratha and Joshi, 2013) and *Nyctanthes arbor-tristis* (Parijat; Night-flowering jasmine), a popular medicinal plant with anti-helminthic and anti-pyretic properties among others were collected (Agrawal & Pal, 2013). The leaves were washed 2-3 times thoroughly with tap water to remove all the dust and unwanted visible particles and then dried at room temperature for few days. The leaves were then grinded to powder and used.

2.2 Preparation of Aqueous extracts of plants and AgNO₃ stock solution

For preparation of aqueous extracts, the method by Banerjee et al., was followed with little modifications. About 10 g of these finely incised leaves of each plant type were weighed separately and transferred into 250 mL beakers containing 100 mL distilled water and boiled for about 5-10 min at 70°C. The extracts were kept aside overnight followed by filtration through muslin cloth to remove particulate matter and to get clear solutions which were then refrigerated (4°C) in 250 mL Erlenmeyer flasks for further experiments (Banerjee et al., 2014). From 100mM stock solution of silver nitrate (AgNO₃) 1mM and 2mM AgNO₃ solution was prepared.

2.3 Optimization of the plants extracts and the pH

A series of three test tubes were filled with varied amounts of aqueous plant extract of *Nyctanthes arbor-tristis* and 1mM AgNO₃ solution in three different ratios of 4:1, 3:2 and 2:3, the same ratios were followed with 2mM of AgNO₃ solution and total of six tubes were prepared. The same method was followed for *Terminalia chebula* as well. The pH of the solutions in each test tubes were checked. A lime yellow indicated a pH of 7. The color is also observed in the remaining test tubes as green, dark green and pale blue which indicates the pH-8, 9 respectively.

2.4 Biosynthesis of silver nanoparticles

After optimization, the optimized ratio is prepared in bulk for the synthesis of nanoparticle. For *Nyctanthes arbor-tristis*, 80ml of extract is mixed with 20ml of 1mM AgNO₃ solution and for *Terminalia chebula*, 60ml of extract is mixed with 40ml of 1mM AgNO₃ solution i.e., in 4:1 ratio. The pH was adjusted to 8. The tubes were heated for 5-10 min in water bath then kept in dark and the color change in each tube is examined and reported after 8 h incubation at room temperature. This is followed by centrifugation at maximum speed. The pellets obtained contains the nanoparticles, which are then dried. To the dried Nanoparticles Dimethyl sulfoxide (DMSO) is added and used for further testing.

2.5 Characterization of silver nanoparticles using

2.5.1 UV-visible spectrophotometry

One of the most used methods for characterizing synthesized nanoparticles is UV-vis spectrophotometry, which is also used to track the stability and production of Ag NPs. Furthermore, UV-vis spectrophotometry is uncomplicated, quick, sensitive, as well as selective for many kinds of nanoparticles (Leung et al., 2006; Huang et al., 2007). It entails calculating how much UV or visible light a substance in solution has absorbed. In the UV-Visible zone, UV-vis determines the ratio or function of ratio, of the intensity of two light beams. The valence band and conduction band of Ag NPs are relatively close to one another, allowing for unrestricted electron mobility. These electrons oscillate collectively in resonance with the input light wave (Noginov et al., 2007; He et al., 2022) to generate a surface plasmon resonance (SPR) band. The dielectric medium, morphology, shape, size, and chemical surroundings of synthesized nanoparticles all affect the absorption spectra of Ag NPs (Link and El-Sayed, 2003). Numerous studies have demonstrated that Ag NPs create absorption bands in the UV-visible spectrum at around 200-800 nm and may be utilized to characterize nanoparticles with a size range of 2-100 nm.

2.5.2 Scanning electron microscope (SEM)

In terms of distinct particle forms, surface morphology, sizes, and size distributions of synthesized nanoparticles at the micro (10⁻⁶) and nano (10⁻⁹) scales, SEM is one of a number of electron microscopy techniques. In SEM, a high intensity electron beam is used to scan over the Ag NPs sample's surface, and backscattered electrons are then observed to reveal the sample's distinctive features (Buhr et al., 2009). To determine the elemental composition of an Ag NPs sample, Energy Dispersive X-Ray Spectroscopy (EDX) is a chemical analysis technique that is utilized in conjunction with SEM (Anandalakshmi et al., 2016). When a sample is bombarded by an electron beam, the EDS approach detects x-rays that are released, and an EDS x-ray detector measures the relative abundance of discharged x-rays in relation to their energy (Pasricha et al., 2009). SEM has the limitation that it cannot examine the sample's internal structure, although it can provide insightful data on the degree of particle aggregation and purity.

2.6 Antioxidant assay

2.6.1 FRAP assay (Ferric reducing antioxidant power):

Following the method developed by Benzie & Strain, the antioxidant capacity of the medicinal plants was calculated spectrophotometrically. The process is based on the reduction of the colourless Fe^{3+} TPTZ complex to blue Fe^{2+} -tripyridyltriazine complex generated by the action of low pH antioxidants that donate electrons (Benzie et al., 1996). The change in absorbance at 420 nm is used to track the progress of this process. At 37°C, 0.25 mM acetate buffer, 10 mM TPTZ, and 20 mM $\text{FeCl}_3 \cdot 6\text{H}_2\text{O}$ were combined to create the ferric reducing antioxidant power (FRAP) reagent.

3 ml of freshly prepared working FRAP reagent was mixed with a range of 50-100 μl of the plant extract and silver nanoparticles (Ag NPs) then mixed thoroughly. An intense blue colour complex was formed when the ferric tripyridyl triazine (Fe^{3+} TPTZ) complex was reduced to ferrous (Fe^{2+}) form and the absorbance at 420 nm was recorded against a reagent blank (3 ml FRAP reagent + 500 μl distilled water) after 5 min incubation at 37°C. The calibration curve was prepared by plotting the absorbance at 420 nm versus different concentrations of FeSO_4 . Frap was expressed as Fe^{2+} equivalents (μM) or FRAP value.

2.6.2 Phosphomolybdate assay

The method for phosphomolybdate assay was used from Umamaheswari & Chatterjee with few modifications. The total antioxidant capacity of the fractions can also be determined by phosphomolybdate method using ascorbic acid as a standard. Aliquots in the range of 50-100 μl of sample solution was mixed with 1ml of reagent solution (0.6ml sulphuric acid, 28mM sodium phosphate and 4mM ammonium molybdate). The tubes were capped and incubated in a water bath at 75°C for 30 mins, followed by incubation at room temperature for 60 mins. After the samples had cooled to room temperature the absorbance of the mixture was measured at 570nm against a blank. A typical blank contained 1ml of the reagent solution and the appropriate volume of the solvent and incubated under same conditions. Ascorbic acid was used as standard (Umamaheswari et al., 2007; Baig et al., 2011) The antioxidant capacity was estimated using following formula:

$$\text{Antioxidant effect\%} = \left[\frac{\text{control absorbance} - \text{sample absorbance}}{\text{control absorbance}} \right] * 100.$$

2.7 Antimicrobial activity

The antimicrobial activity of the biosynthesized Ag NPs extract, AgNO_3 and standard antibiotic were examined using a disk diffusion assay for both antibacterial and anti-fungal activities.

2.7.1 Antibacterial activity testing by Agar Well Disc Diffusion Method

Muller hinton agar was prepared according to the requirement by dissolving in distilled water and heated to boil to dissolve the medium completely, then sterilized by autoclaving at 15lbs pressure (121°C) for 15 minutes, cooled to 45-50°C, mixed well and poured into sterile Petri plates.

The comparative antibacterial activity of the plant extracts and Ag NPs synthesized by *Nyctanthes arbor-tristis* and *Terminalia chebula* were effectively accessed against, two Gram (-) ve (*Escherichia coli* (*E. coli*), *Klebsiella*) bacteria and two Gram (+) ve (*Bacillus* and *staphylococcus*) bacteria as test microorganisms. Disc diffusion method (Ghaffari-Moghaddam et al., 2014) was followed for testing each type of plant leaf extract and their respective Ag NPs containing solution. Pure cultures of bacteria were cultured on nutrient broth medium at 37°C and incubated overnight. The bacteria were then swabbed on the MH agar plates using a cotton swab. Wells of size 8 mm have been made on Muller–Hinton agar plates using gel puncture. The extracts in the range of 50µl, 100µl and Ag NPs in the range of 25µl, 50µl, 75µl and 100µl, AgNO₃ and DMSO were filled in the wells using micropipette, antibiotic was used a positive reference control to determine the sensitivity of each bacterial species. Then the plates were incubated overnight in the incubator at 37 °C. Then, the maximum zone of inhibition was observed and measured for analysis against each type of test microorganism (Banerjee et al., 2014).

2.7.2 Antifungal activity testing by Agar Well Disc Diffusion Method

Potato dextrose agar was prepared according to the requirement by dissolving in distilled water and heated to boil to dissolve the medium completely, then sterilized by autoclaving at 15lbs pressure (121°C) for 15 minutes, cooled to 45-50°C, mixed well and poured into sterile Petri plates.

Disc diffusion method (Ghaffari-Moghaddam et al., 2014) was followed for performing antifungal activity for plant extracts and Ag NPs. The activity was determined against the *Aspergillus niger*. The fungi were swabbed on the potato dextrose agar plates using sterilized cotton swab. Wells of size 8 mm have been made on Muller–Hinton agar plates using gel puncture. Then extracts in the range of 50µl, 100µl and Ag NPs in the range of 25µl, 50µl, 75µl, and 100µl were filled using micropipette in sterile disc or wells. Activity was determined after about a week of incubation, then zones were measured using in ordinary scale.

2.8 Study of catalytic activity of biosynthesized silver nanoparticles against methylene blue and malachite green

The protocol by Singh & Dhaliwal was followed with some modifications, typically, 0.5mg of methylene blue dye and malachite green was added to 50ml of distilled water and used as working standard solution. Aliquots ranging from 20-100µl of biosynthesized nanoparticles of both plant extract samples were taken in series of tubes. 3ml of methylene blue dye (50 ppm) and malachite green (50 ppm) was added in all the tubes. A control was also maintained without addition of silver nanoparticles. Before exposing to irradiation, the reaction suspension was well mixed to clearly make the equilibrium of the working solution. Afterwards, the dispersion was put under the sunlight and monitored for 72 hours. At specific time intervals, aliquots of 2-3ml of suspension were taken and used to elevate the photo catalytic degradation of dye. The absorbance spectrum was subsequently measured using UV visible spectrophotometer. Concentration of dye during degradation was calculated by the absorbance value at 490nm (Singh and Dhaliwal, 2020).

Percentage of dye degradation was estimated by the following formula

$$\% \text{ Degradation} = \frac{C_o - C_t}{C_o} \times 100$$

C_o

Where,

C_o is the initial concentration of dye solution.

C_t is the concentration of dye solution after photo catalytic degradation.

3. RESULTS

3.1 Synthesis of silver nanoparticles: Process optimization and UV characterization

Aqueous plant extracts of *Nyctanthes arbor-tristis* and *Terminalia chebula* were used in the reduction of AgNO_3 into Ag^0 , and the reduction was initially confirmed by the color change from colorless to yellowish brown (Rajeshkumar and Bharath, 2017). The UV-visible spectral analysis of the extract with AgNO_3 solution showed maximum absorbance at 450 nm as the characteristic surface plasmon resonance (SPR) peak of Ag NPs. The formation of SPR peak is influenced by various factors such as size, shape and particles formed.

The extract concentration of 10% of *Nyctanthes arbor-tristis* and *Terminalia chebula* plant extracts in deionized water, AgNO_3 concentration 1.0 mM, reaction time of 5-10 min, pH 8.0 and temperature at 70°C were the optimized condition for the synthesis of Ag NPs. After optimization of pH and temperature (pH 8.0 and 70°C), the time period for nanoparticle formation after incubation in the dark was 8 h.



Fig. 1. Plant extracts of (a) *Terminalia chebula*, (b) *Nyctanthes arbor-tristis*.

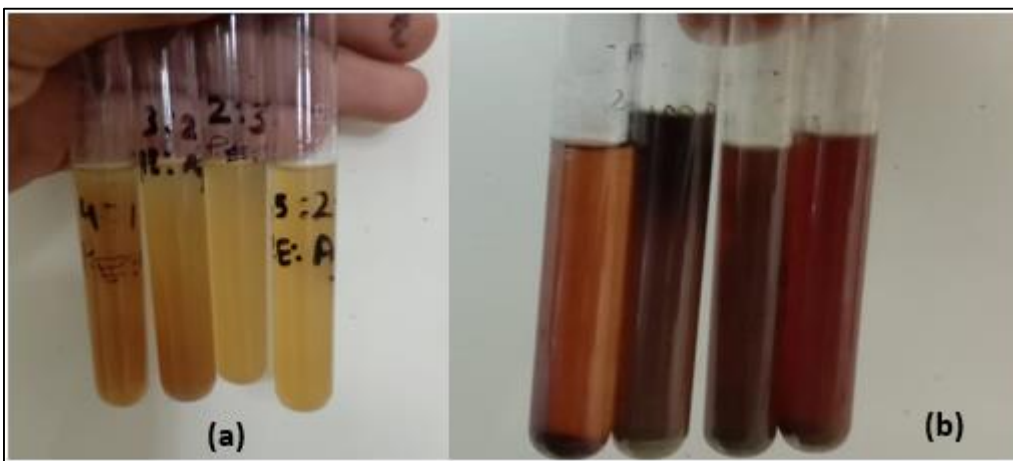
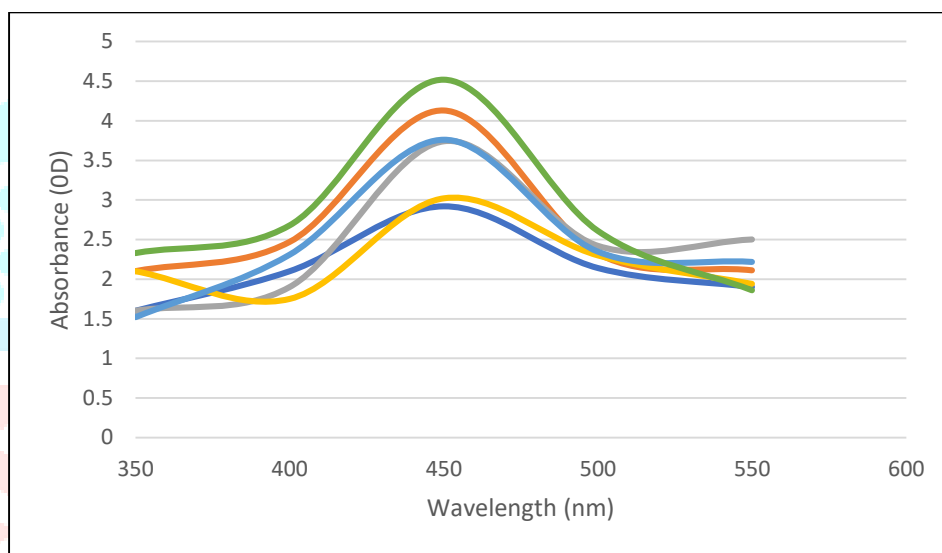
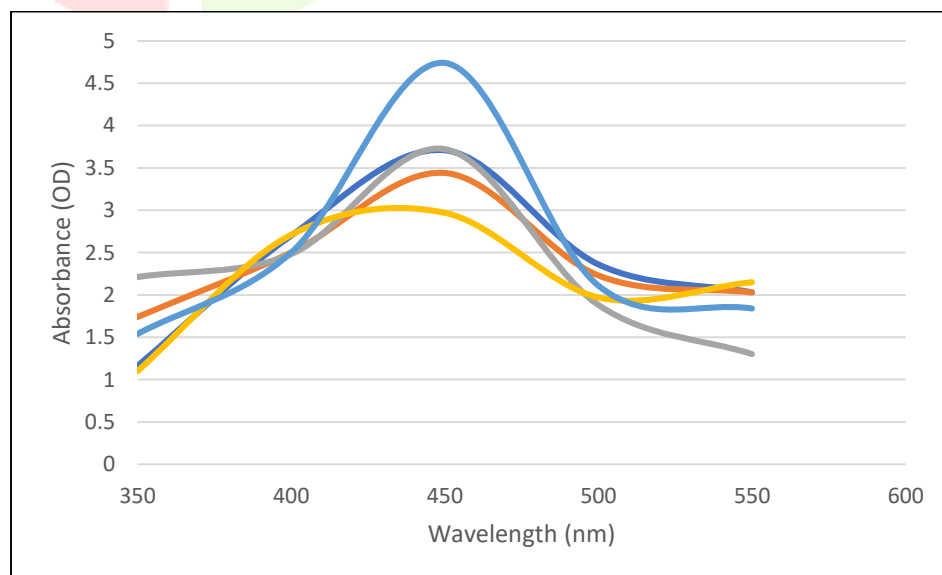


Fig. 2. Process optimization for synthesis of silver nanoparticles (a) Before heating the different ratios of Plant extracts and AgNO₃; (b) After heating.



(a)



(b)

Fig. 3. UV-vis spectra of silver nanoparticles synthesized by (a) *Nyctanthes arbor-tristis* extract (b) *Terminalia chebula* show the SPR band at 450 nm and could confirm the formation of silver nanoparticles in the reaction mixture.

3.2 Characterization of silver nanoparticles by SEM

The scanning electron microscopy (SEM) image of synthesized AgNPs showed that the particles synthesized using leaf extract of *Nyctanthes arbor-tristis* were spherical in shape and monodispersed with varying sizes from 29.49 to 266.5 nm in diameter with an average size of 88.5 nm (Fig.4b). Whereas those from *Terminalia chebula* were nanorods (Wahab et al., 2016) with varying sizes from 142.5 nm - 6.372 μm in diameter (Fig.4a). Sizes and shapes of metal nanoparticles are affected by various factors including pH, time of incubation, precursor concentration, reductant concentration, temperature as well as method of preparation. The distribution, toxicity, and targeting capabilities of nanoparticles are determined by their size and form, which also impacts how cells in the body "see" them (McMillan et al., 2011). The optimum size for a nanoparticle is approximately 100 nm. It has been reported that 100 nm nanoparticles exhibited a 2.5-fold greater uptake compared to 1 μm diameter particles and a 6-fold greater uptake than a 10 μm particles (Desai et al., 1997).

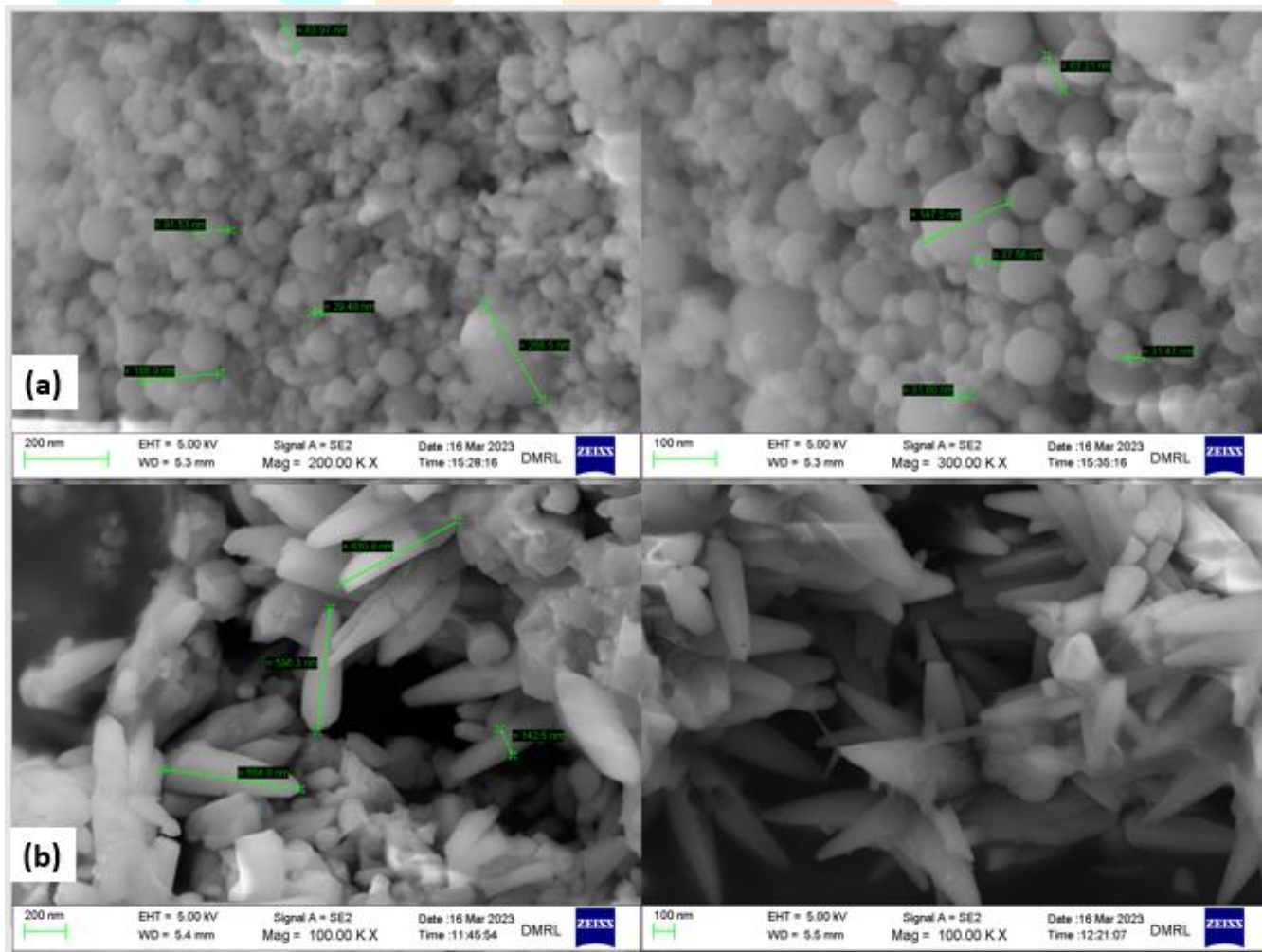


Fig. 4. SEM images of silver nanoparticles. Formed from silver nitrate and leaf extract of (a) *Terminalia chebula* (b) *Nyctanthes arbor-tristis*.

3.3 Antioxidant Assay

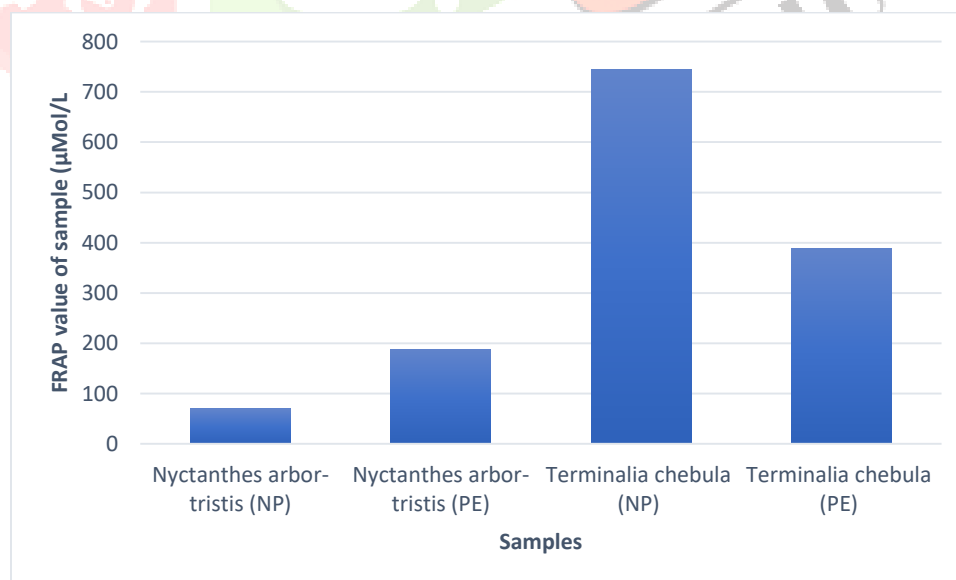
3.3.1 FRAP assay (Ferric reducing antioxidant power):

3 ml of freshly prepared working FRAP reagent was mixed with a range of 50-100 μ l of the plant extract and silver nanoparticles (Ag NPs) then mixed thoroughly. the absorbance at 420 nm was recorded against a reagent blank (3 ml FRAP reagent + 500 μ l distilled water) after 5 min incubation at 37°C.

Table 1

Reducing power by FRAP assay, Total antioxidant activity by phosphomolybdate assay.

S. No	Extract	FRAP value of sample (μ Mol/L)	Total antioxidant effect (%)
1	<i>Nyctanthes arbor-tristis</i> (NP)	70	81.76%
2	<i>Nyctanthes arbor-tristis</i> Plant extract	187.78	57.12%
3	<i>Terminalia chebula</i> (NP)	745.56	33.44%
4	<i>Terminalia chebula</i> Plant extract	387.78	85.28%

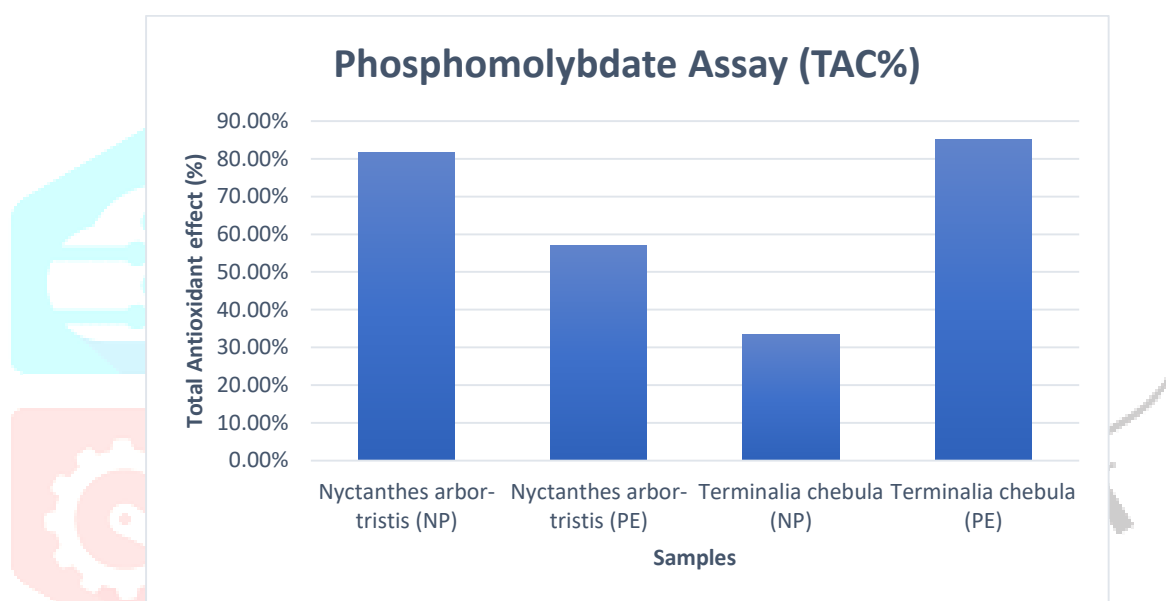


Graph 1: FRAP value of *Nyctanthes arbor-tristis* nanoparticle (NP) & plant extract (PE) and *Terminalia chebula* nanoparticle (NP) & plant extract (PE).

In FRAP assay, a pigmented complex of ferrous tripyridyltriazine (Fe^{2+} - TPTZ) is produced when an antioxidant reacts with a ferric tripyridyltriazine (Fe^{3+} - TPTZ) complex, which assesses the reducing potential of an antioxidant. The results of the FRAP assay in terms of FRAP value in $\mu\text{Mol/L}$ related to single electron transfer reducing (antioxidant) capacity as represented by the Fe^{2+} standard is shown in Table 1. The *Terminalia chebula* NPs showed good reducing activity ($745.56 \mu\text{Mol/L}$ of FeSO_4 equivalent). The ability of the samples to reduce iron (III) to iron(II) decreases in the order of *Terminalia chebula* NPs > *Terminalia chebula* PE > *Nyctanthes arbor-tristis* PE > *Nyctanthes arbor-tristis* NPs.

3.3.2 Phosphomolybdate assay

The total antioxidant activity of plant extract and silver nanoparticles was estimated by phosphomolybdate assay by using ascorbic acid as the standard.



Graph 2: Total Antioxidant effect (%).

Phosphomolybdate assay is based on the reduction of molybdenum (VI) to molybdenum (V) that occurs in the presence of a reducing substance (antioxidant). A spectrophotometer is used to track the formation of the end result, a green phosphomolybdate(V) compound. The assay is frequently used to calculate the overall antioxidant activity of a material, and the findings are stated in percentage of TAC. The overall antioxidant activity of different samples declines in the following order: *Terminalia chebula* PE > *Nyctanthes arbor-tristis* NPs > *Nyctanthes arbor-tristis* PE > *Terminalia chebula* NPs.

3.4 Antimicrobial activity

3.4.1 Antibacterial activity testing by Agar Well Disc Diffusion Method

The antimicrobial activity of silver nanoparticles synthesized by natural plants extract was investigated against various pathogenic organisms such as *Escherichia coli* (*E. coli*) and *Bacillus* using well diffusion method. The diameter of inhibition zones (mm) around each well with silver nanoparticles solution and the plant extracts is

represented in Table 2. Ciprofloxacin was used as an antibiotic (Terp & Rybak, 1987). The silver nanoparticles synthesized by *Terminalia chebula* and *Nyctanthes arbor-tristis* extracts were found to have high antimicrobial activity against *Bacillus* and lesser antimicrobial activity against *E. coli* (Table. 2). Due to their incredibly huge surface area, which allows for better interaction with microbes, the silver nanoparticles demonstrated good antibacterial capability in comparison to other salts. The nanoparticles enter the bacteria's cell wall and get linked to it. Silver nanoparticles interact with sulfur-containing proteins found in the bacterial membrane as well as phosphorus-containing substances like DNA in the cell. The DNA is protected from the silver ions when silver nanoparticles enter the bacterial cell because they create a low molecular weight zone in the core of the bacterium. Preferably, the respiratory chain is the target of the nanoparticles, and cell division ultimately results in cell death. In the bacterial cells, the nanoparticles release silver ions, enhancing their bactericidal effect (Morones et al., 2005).

Table 2

Zone of inhibition (mm) of silver nanoparticles synthesized by natural plant extracts against various pathogenic bacteria

Extracts	Bacteria	Zone of Inhibition (in mm)			
		by NPs			By Antibiotic (Ciprofloxacin)
		50µL	100 µL	150 µL	
<i>Terminalia chebula</i>	+ (<i>Bacillus</i>)	7	7	8.5	10
	- (<i>E. Coli</i>)	5	6	7	7.5
<i>Nyctanthes Arbor-Tristis</i>	+ (<i>Bacillus</i>)	2.5	4	9	8
	- (<i>E. Coli</i>)	2.5	3.5	6.5	9

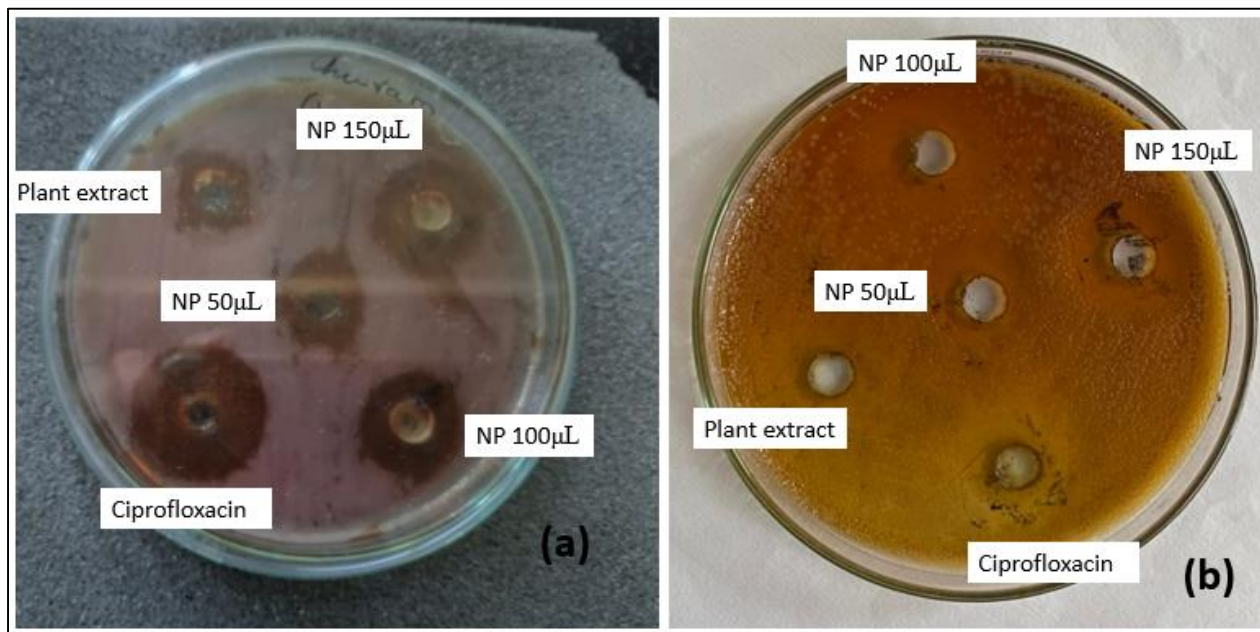


Fig. 5. Zone of inhibition by *Terminalia chebula* against (a) gram (+) *Bacillus* and (b) gram (-) *E Coli*.

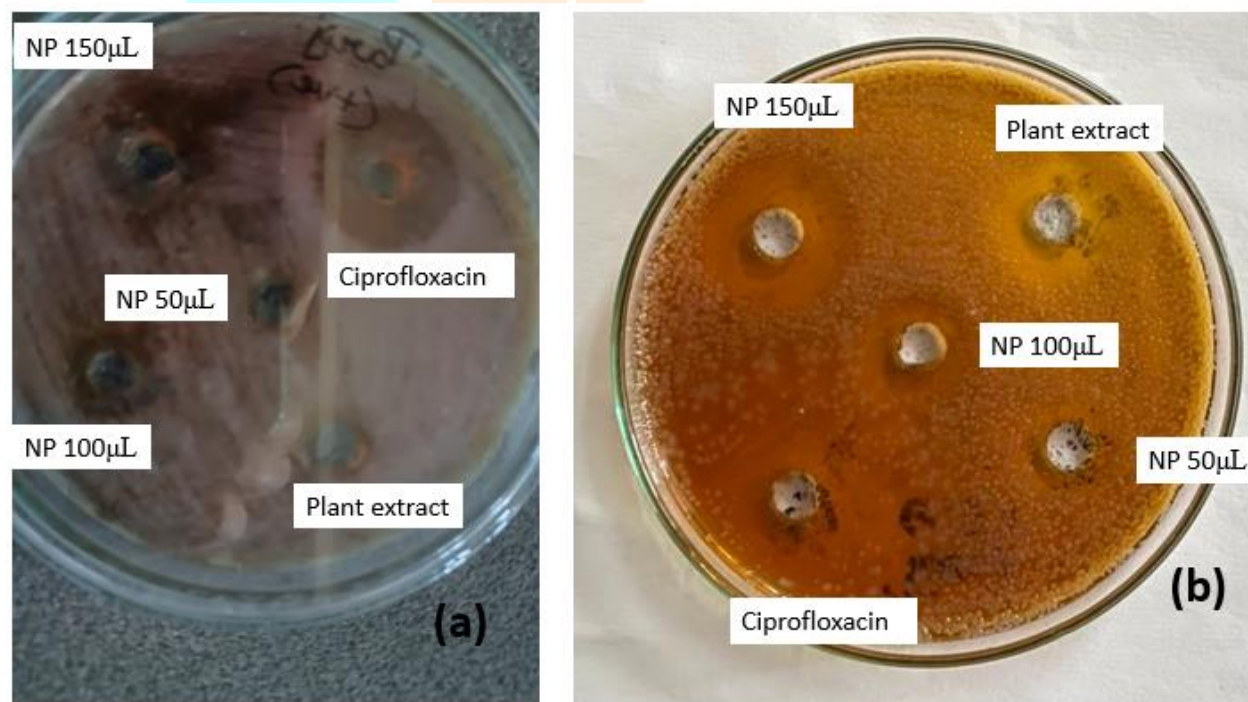


Fig. 6. Zone of inhibition by *Nyctanthes arbor-tristis* against (a) gram (+) *Bacillus* and (b) gram (-) *E Coli*

3.4.2 Antifungal activity testing by Agar Well Disc Diffusion Method

Antifungal activity was performed for *Terminalia chebula* and *Nyctanthes arbor-tristis* plant extracts and AgNPs, and zone of inhibition was determined against *Aspergillus niger*. Fluconazole was used as an antifungal medicine (Richardson et al., 1990). The activity was determined after 1 week of incubation at 37°C. The diameter of inhibition zones was observed.

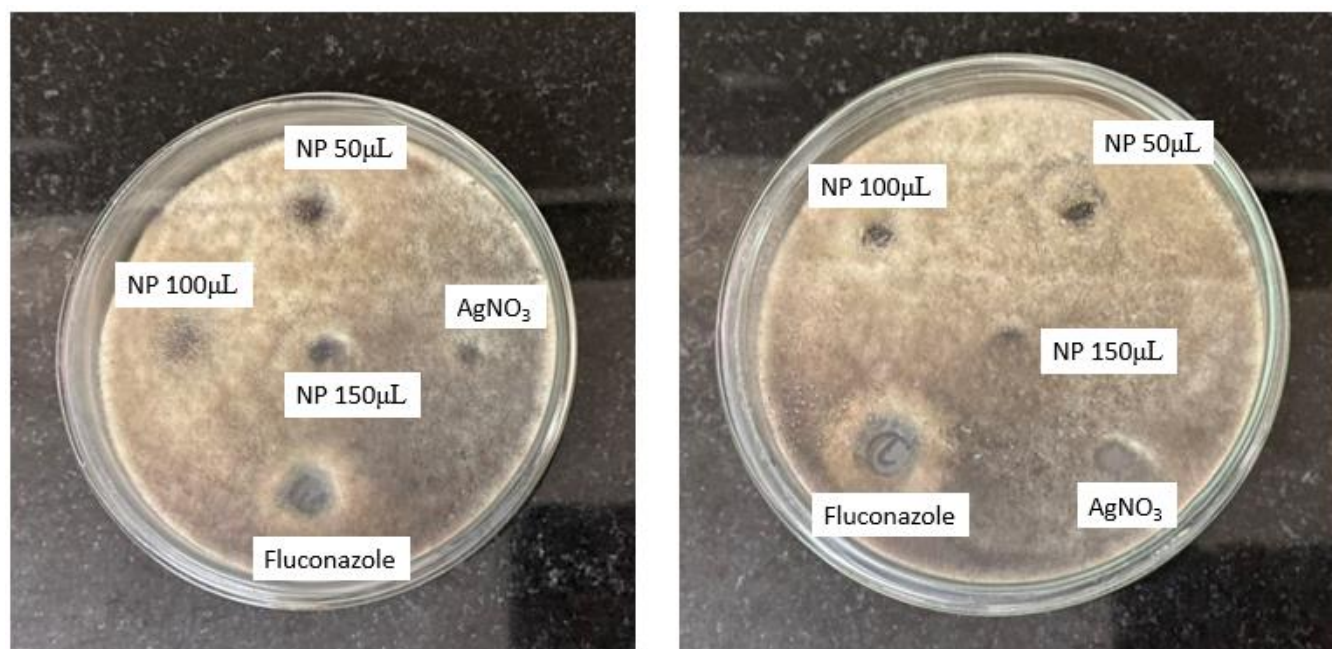


Fig. 7. Zone of inhibition by *Terminalia chebula* and *Nyctanthes arbor-tristis* respectively against *Aspergillus niger*.

3.5 Study of catalytic activity of biosynthesized silver nanoparticles against methylene blue and malachite green

The photocatalytic degradation of malachite green and methylene blue dye by using synthesized silver nanoparticles is studied in the presence of sunlight and absence of sunlight. The change in color of the test tubes from a dark shade of green to a lighter shade, in case of malachite green and from a dark shade of blue to a lighter one as shown in the Fig.8, 9 indicates the degradation of Malachite green and methylene blue in the presence of AgNP.

The percentage of catalytic degradation of malachite green and methylene blue at different concentration in the presence of light has been shown in the (Graph.3), for a given time interval (24 h) and concentration of methylene blue (50 ppm) and malachite green (50 ppm) (Singh & Dhaliwal, 2020).

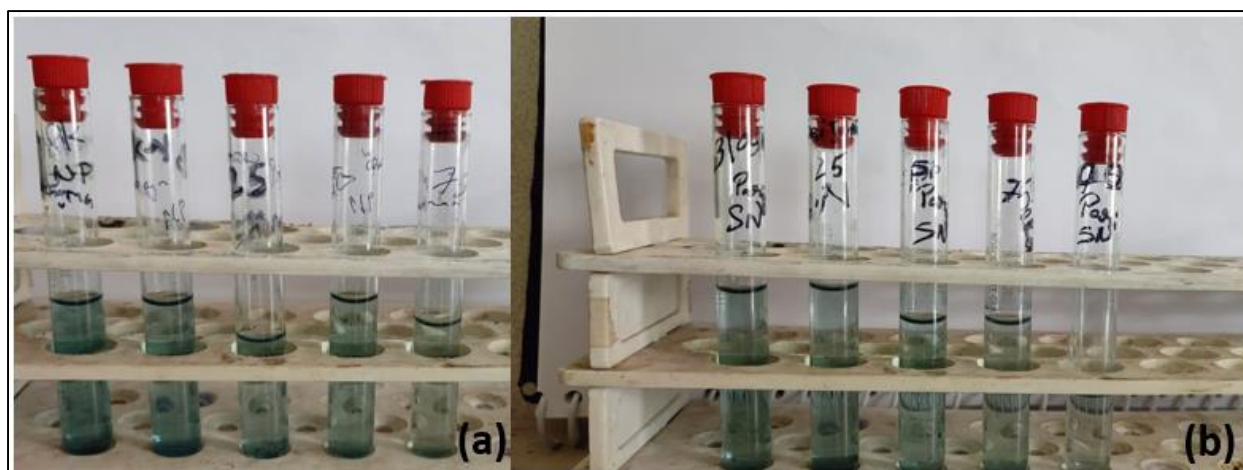


Fig. 8. Photocatalytic reduction of Malachite green by *Nyctanthes arbor-tristis* synthesized silver nanoparticles before and after exposure to sunlight.

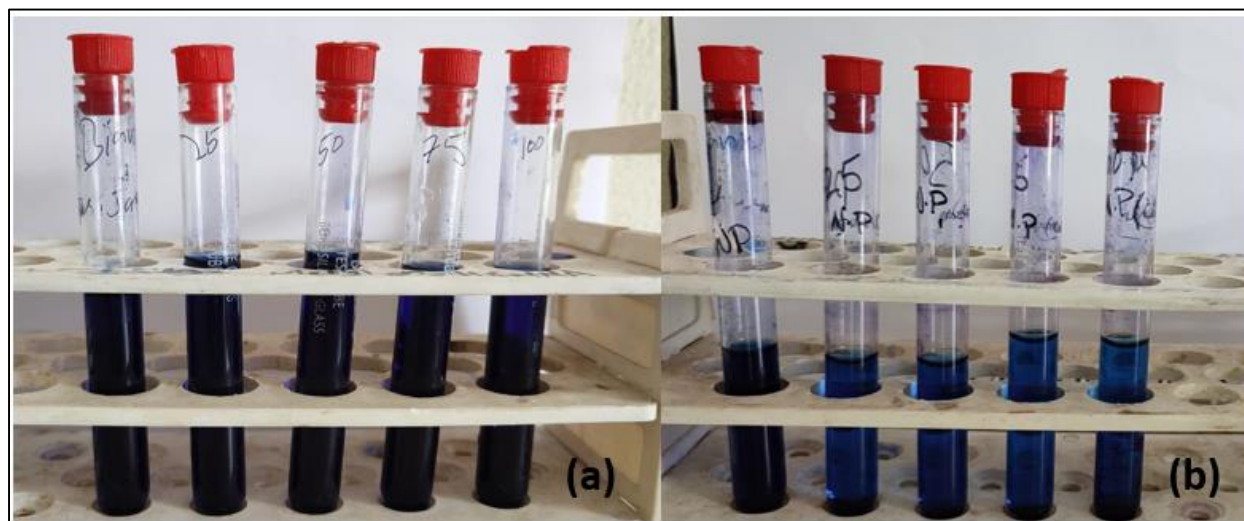
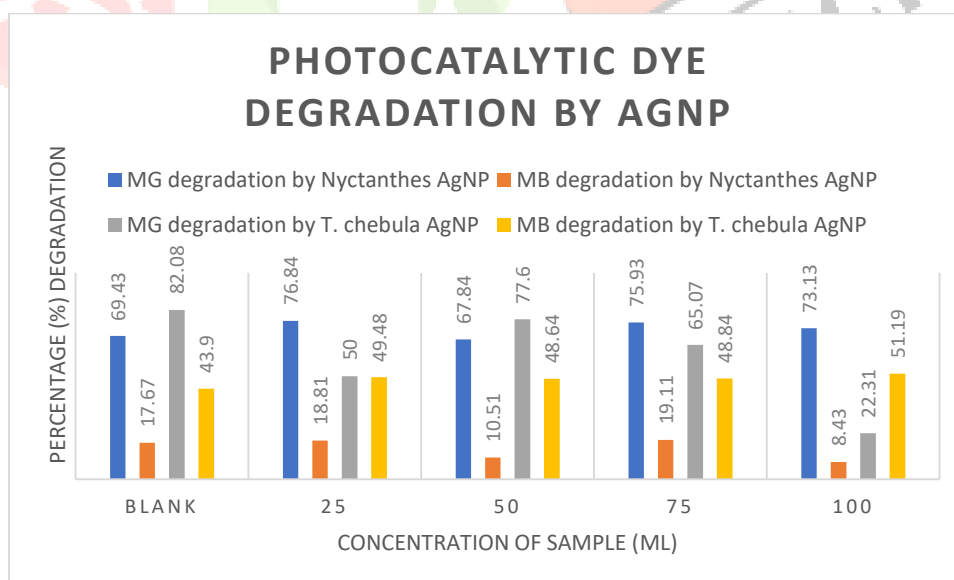


Fig. 9. Photocatalytic reduction of Methylene Blue by *Nyctanthes arbor-tristis* synthesized silver nanoparticles before and after exposure to sunlight.

The photocatalytic degradation of methylene blue and malachite green dye was investigated using synthesized silver nanoparticles as photocatalyst. Silver nanoparticles absorb visible light due to Surface Plasmon Effect and used as plasmonic photocatalyst. There was considerable degradation of methylene blue dye than malachite green by both AgNPs. Hence, from the present work, it may be concluded that the biosynthesized silver nanoparticles may be used as promising catalyst for the effective photocatalytic degradation of methylene blue and malachite green from aqueous solution.



Graph 3: Photocatalytic degradation of dye (%) by silver nanoparticles at different concentrations.

DISCUSSION

There are numerous possible uses for green nanoparticle synthesis in the health and environmental sciences. Green synthesis specifically seeks to reduce the use of harmful substances. For instance, it is typically acceptable to use biological elements like vegetation. Reducers and caps are also present in plants. It has been suggested that a more affordable and ecologically responsible technique for creating nanoparticles than chemical and physical processes is biosynthesis. An environmentally friendly method of creating nanomaterials that integrates plants and nanotechnology is called plant-mediated synthesis. Thus, novel strategies for creating NPs that are produced at room temperature, with a neutral pH, at low expense, and in an ecologically benign manner are being considered (Mohanpuriya et al., 2008).

In the present work, we reported a simple, ecofriendly and cost-effective method for the green synthesis of silver nanoparticles using two plant extracts *Terminalia chebula* and *Nyctanthes arbor-tristis*. The biosynthesized nanoparticles were characterized using various analytical methods such as UV-vis spectroscopy, SEM. Antimicrobial and antioxidant activity of the AgNPs synthesized from *Terminalia chebula* and *Nyctanthes arbor-tristis* were also analyzed.

Sharma et al reported the formation of AgNPs from leaf extract of *Nyctanthes* from UV-vis spectroscopy, at a range of 450-48nm (Sharma et al., 2021). Another study for the rapid green synthesis of AgNP using *Terminalia chebula* aqueous extract was reported in 2012. The SPR band was observed at 452 nm (Mohan et al., 2012). Our presented work is in coherence with the above studies, we diluted our sample with certain amount and scanned in a UV-vis spectrometer with quartz cuvettes between 350nm and 650nm, the Fig.3 shows the absorption spectra of the silver nanoparticles with two different leaf extracts, the peak was observed at 450 nm for both plant extracts. Generally, the wavelength of Ag-NPs resonance absorption peak is in the range of 400–500 nm. The observation clearly indicated the successful synthesis of silver nanoparticles.

Sharma et al., also reported the formation of AgNPs using leaf extract of *Nyctanthes arbor-tristis* with size range of 40-60nm (Sharma et al., 2021). In our study we also reported the scanning electron microscopy (SEM) image of synthesized AgNPs showing that the particles synthesized using leaf extract of *Nyctanthes arbor-tristis* being spherical in shape and monodispersed with varying sizes from 29.49 to 266.5 nm in diameter with an average size of 88.5 nm.

In 2013, Michael and his colleague investigated the in vitro antioxidant activity and total phenolic content of methanolic leaf extract of *N. arbor-tristis*, their results reported potent free radical scavenging activity indicating *N. arbor-tristis* to be a potent source of natural antioxidant (Michael et al., 2013). Kathirvel & Sujatha conducted a study to access the antioxidant activity from the leaves of *Terminalia chebula* and reported it as a good source of natural antioxidants (Kathirvel & Sujatha et al., 2013). In our study, we conducted FRAP and phosphomolybdate assay and found *T. chebula* NPs and Plant extract to be showing good antioxidant activity (745.56 $\mu\text{Mol/L}$, 387.78 $\mu\text{Mol/L}$ of FeSO_4 equivalent respectively). Total antioxidant capacity % (TAC%) as calculated through phosphomolybdate assay showed antioxidant activity of different samples in the following

order: Terminalia chebula PE (85.28%) > *Nyctanthes arbor-tristis* NPs (81.76%) > *Nyctanthes arbor-tristis* PE > Terminalia chebula NPs.

Due to the ongoing rise in microbial illnesses and disorders, as well as ineffective treatments, metallic nanoparticles such as silver nanoparticles (AgNPs) have drawn a lot of attention. Additionally, due to the fast increase of antibiotic resistance during this time, scientists and scholars are once again considering investigating the therapeutic potential of silver and its nanoparticulate systems as possible antimicrobial agents. AgNPs have been shown to have substantial antimicrobial effects, particularly against bacterial illnesses, according to numerous studies. Sharma et al, reported that synthesized AgNPs from aqueous leaf extract of *N. arbor-tristis* showed effective antimicrobial efficiencies against *Escherichia coli* (*E. coli.*), *Staphylococcus aureus* (*S. aureus*) and *Shewanella putrifaction* (*S. putrifaction*) (Sharma et al., 2021). In our results of antimicrobial activity was also found to be in coherence with these previous studies with the nanoparticles synthesized from the leaf extract of both the plants demonstrating potent activity against gram-positive *Bacillus* and gram-negative *E. coli*.

It has been reported by Khan et al., that aqueous, alcoholic and ethyl acetate extracts of *T. chebula* shows antifungal activity against *Aspergillus niger* (Khan et al., 2015). Jamdagni and his colleagues synthesized zinc oxide nanoparticles using flower extract of *Nyctanthes arbor-tristis*. They observed potent antifungal activity of the nanoparticles against all the tested phytopathogens including *Aspergillus niger* (Jamdagni et al., 2018). However, in our study no results regarding antifungal activity of silver nanoparticles synthesized from the two plants were observed.

Sharma et al., in the year 2023 reported the *Nyctanthes* based AgNPs exhibited efficient catalytic activity in NaBH₄ mediated reduction of mordant orange- 1 (MO-1) and methylene blue (MB). The results showed that Nyc.-AgNPs degraded more than 80% to both dyes (Sharma et al., 2023) Our study reported the photocatalytic degradation of two dyes methylene blue and malachite green by the green synthesized NPs from the two plants (Graph.3), with Nyc.-AgNPs and *T. chebula*-AgNPs showing an average degradation of 73.43% and 53.75% respectively, for Malachite green and an average of 14.21% and 49.53% degradation for Methylene blue by *Nyctanthes arbor-tristis* and *T. chebula* AgNP indicating that it could be a potent candidate for treatment of contaminated water.

CONCLUSION

In the present study, we reported a simple, ecofriendly and cost-effective method for the green synthesis of silver nanoparticles from the leaves of Terminalia chebula and *Nyctanthes arbor-tristis*. Furthermore, the biosynthesized nanoparticles were characterized using various analytical methods such as UV-vis spectroscopy, SEM. Antimicrobial and antioxidant activity of the AgNPs synthesized from Terminalia chebula and *Nyctanthes arbor-tristis* were also analyzed. However, good antibacterial activity by the synthesized nanoparticles was

observed but no antifungal activity. The results of the above study yielded good results providing potential applications in the field of medicine.

References :

- J. Agrawal, & A. Pal, *Nyctanthes arbor-tristis* Linn--a critical ethnopharmacological review, *Journal of ethnopharmacology*. 146 (2013) 645–658. <https://doi.org/10.1016/j.jep.2013.01.024>
- K. Anandalakshmi, J. Venugobal, & V. J. A. N. Ramasamy, Characterization of silver nanoparticles by green synthesis method using *Petalium murex* leaf extract and their antibacterial activity, *Applied nanoscience*. 6 (2016) 399-408. doi:10.1007/s13204-015-0449-z
- H. Baig, D. Ahmed, S. Zara, M. I. Aujla, & M. N. Asghar, In vitro evaluation of antioxidant properties of different solvent extracts of *Rumex acetosella* leaves, *Oriental journal of chemistry*. 27 (2011) 1509.
- P. Banerjee, M. Satapathy, A. Mukhopahayay, & P. Das, Leaf extract mediated green synthesis of silver nanoparticles from widely available Indian plants: synthesis, characterization, antimicrobial property and toxicity analysis, *Bioresources and Bioprocessing*. 1 (2014) 1-10. <https://doi.org/10.1186/s40643-014-0003-y>
- I. F. Benzie, & J. J. Strain, The ferric reducing ability of plasma (FRAP) as a measure of "antioxidant power": the FRAP assay, *Analytical biochemistry*. 239 (1996) 70–76. <https://doi.org/10.1006/abio.1996.0292>
- E. Buhr, N. Senftleben, T. Klein, D. Bergmann, D. Gnieser, C. G. Frase, & H. Bosse, Characterization of nanoparticles by scanning electron microscopy in transmission mode, *Measurement science and Technology*. 20 (2009) 084025. doi:10.1088/0957-0233/20/8/084025
- M. P. Desai, V. Labhasetwar, E. Walter, R. J. Levy, & G. L. Amidon, The mechanism of uptake of biodegradable microparticles in Caco-2 cells is size dependent, *Pharmaceutical research*. 14 (1997) 1568–1573. <https://doi.org/10.1023/a:1012126301290>
- L. Ge, Q. Li, M. Wang, J. Ouyang, X. Li, & M. M. Xing, Nanosilver particles in medical applications: synthesis, performance, and toxicity, *International journal of nanomedicine*. 9 (2014), 2399–2407. <https://doi.org/10.2147/IJN.S55015>
- M. Ghaffari-Moghaddam, R. Hadi-Dabanlou, M. Khajeh, M. Rakhshanipour, & K. Shameli, Green synthesis of silver nanoparticles using plant extracts, *Korean Journal of Chemical Engineering*. 31 (2014) 548-557. doi:10.1007/s11814-014-0014-6
- R. He, X. Qian, J. Yin, & Z. Zhu, Preparation of polychrome silver nanoparticles in different solvents, *Journal of Materials Chemistry*. 12 (2002) 3783-3786. <https://doi.org/10.1039/B205214H>
- H. Huang, & Y. Yang, Preparation of silver nanoparticles in inorganic clay suspensions, *Composites Science and Technology*. 68 (2008) 2948-2953. <https://doi.org/10.1016/j.compscitech.2007.10.003>
- X. Huang, P. K. Jain, I. H. El-Sayed, & M. A. El-Sayed, Gold nanoparticles: interesting optical properties and recent applications in cancer diagnostics and therapy, *Nanomedicine (London, England)*. 2 (2007) 681–693. <https://doi.org/10.2217/17435889.2.5.681>
- P. Jamdagni, P. Khatri, & J. S. Rana, Green synthesis of zinc oxide nanoparticles using flower extract of *Nyctanthes arbor-tristis* and their antifungal activity, *Journal of King Saud University-Science*. 30 (2018) 168-175. <https://doi.org/10.1016/j.jksus.2016.10.002>

A. Kathirvel, & V. Sujatha, In vitro assessment of antioxidant and antibacterial properties of Terminalia chebula Retz. leaves, Asian Pacific Journal of Tropical Biomedicine. 2 (2012) S788-S795. [https://doi.org/10.1016/S2221-1691\(12\)60314-1](https://doi.org/10.1016/S2221-1691(12)60314-1)

M. U. Khan, H. Khalilullah, J. Akhtar, & G. O. Elhasan, Terminalia chebula: an ephemeral glance, Int J Pharm Pharmac Sci. 7 (2015) 40-43.

A. B. Leung, K. I. Suh, & R. R. Ansari, Particle-size and velocity measurements in flowing conditions using dynamic light scattering, Applied optics. 45 (2006) 2186-2190. <https://doi.org/10.1364/AO.45.002186>

S. Link, & M. A. El-Sayed, Optical properties and ultrafast dynamics of metallic nanocrystals, Annual review of physical chemistry. 54 (2003) 331-366. <https://doi.org/10.1021/jp972807s>

R. Manjumeena, D. Duraibabu, J. Sudha, & P. T. Kalaichelvan, Biogenic nanosilver incorporated reverse osmosis membrane for antibacterial and antifungal activities against selected pathogenic strains: an enhanced eco-friendly water disinfection approach. Journal of environmental science and health. Part A, Toxic/hazardous substances & environmental engineering. 49 (2014) 1125–1133. <https://doi.org/10.1080/10934529.2014.897149>

J. McMillan, E. Batrakova, & H. E. Gendelman, Cell delivery of therapeutic nanoparticles, Progress in molecular biology and translational science. 104 (2011) 563–601. <https://doi.org/10.1016/B978-0-12-416020-0.00014-0>

J. S. Michael, A. Kalirajan, C. Padmalatha, & A. J. Singh, In vitro antioxidant evaluation and total phenolics of methanolic leaf extracts of Nyctanthes arbor-tristis L, Chinese journal of natural medicines. 11 (2013) 484–487. [https://doi.org/10.1016/S1875-5364\(13\)60088-6](https://doi.org/10.1016/S1875-5364(13)60088-6)

K. Mohan Kumar, M. Sinha, B. K. Mandal, A. R. Ghosh, K. Siva Kumar, & P. Sreedhara Reddy, Green synthesis of silver nanoparticles using Terminalia chebula extract at room temperature and their antimicrobial studies, Spectrochimica acta. Part A, Molecular and biomolecular spectroscopy. 91 (2012) 228–233. <https://doi.org/10.1016/j.saa.2012.02.001>

P. Mohanpuria, N. K. Rana, & S. K. Yadav, Biosynthesis of nanoparticles: technological concepts and future applications, Journal of nanoparticle research. 10 (2008) 507-517. doi:10.1007/s11051-007-9275-x

J. R. Morones, J. L. Elechiguerra, A. Camacho, K. Holt, J. B. Kouri, J. T. Ramírez, & M. J. Yacaman, The bactericidal effect of silver nanoparticles, Nanotechnology. 16 (2005) 2346–2353. <https://doi.org/10.1088/0957-4484/16/10/059>

M. A. Noginov, G. Zhu, M. Bahoura, J. Adegoke, C. Small, B. A. Ritzo, V. M. Shalaev, The effect of gain and absorption on surface plasmons in metal nanoparticles, Applied Physics B. 86 (2007) 455-460. doi:10.1007/s00340-006-2401-0

R. Pasricha, T. Bala, A. V. Biradar, S. Umbarkar & M. Sastry, Synthesis of catalytically active porous platinum nanoparticles by transmetallation reaction and proposition of the mechanism, Small. 5 (2009) 1467-1473. <https://doi.org/10.1002/sml.200801863>

S. Rajeshkumar, & L. V. Bharath, Mechanism of plant-mediated synthesis of silver nanoparticles - A review on biomolecules involved, characterisation and antibacterial activity, Chemico-biological interactions. 273 (2017) 219–227. <https://doi.org/10.1016/j.cbi.2017.06.019>

K. K. Ratha, & G. C. Joshi, Haritaki (Chebulic myrobalan) and its varieties, Ayu. 34 (2013) 331–334. <https://doi.org/10.4103/0974-8520.123139>

K. Richardson, K. Cooper, M. S. Marriott, M. H. Tarbit, P. F. Troke, & P. J. Whittle, Discovery of fluconazole, a novel antifungal agent, *Reviews of infectious diseases*. 12 (1990) S267–S271. https://doi.org/10.1093/clinids/12.supplement_3.s267

K. Shamel, M. B. Ahmad, W. M. Yunus, A. Rustaiyan, N. A. Ibrahim, M. Zargar & Y. Abdollahi, Green synthesis of silver/montmorillonite/chitosan bionanocomposites using the UV irradiation method and evaluation of antibacterial activity, *International journal of nanomedicine*. 5 (2010) 875–887. <https://doi.org/10.2147/IJN.S13632>

L. Sharma, M. Dhiman, A. Dadhich, M. M. Sharma, & P. Kaushik, Biogenic AgNPs Synthesized using *Nyctanthes arbor-tristis* L. fruit for antimicrobial & dye degradation efficiencies, *Journal of King Saud University-Science*. (2023) 102614. <https://doi.org/10.1016/j.jksus.2023.102614>

L. Sharma, M. Dhiman, A. Singh, & M. M. Sharma, Biological synthesis of silver nanoparticles using *Nyctanthes arbor-tristis* L.: A green approach to evaluate antimicrobial activities, *Materials Today: Proceedings*. 43 (2021) 2915-2920. <https://doi.org/10.1016/j.matpr.2021.01.208>

J. Singh, & A. S. Dhaliwal, Plasmon-induced photocatalytic degradation of methylene blue dye using biosynthesized silver nanoparticles as photocatalyst, *Environmental technology*. 41 (2020) 1520–1534. <https://doi.org/10.1080/09593330.2018.1540663>

D. K. Terp, & M. J. Rybak, Ciprofloxacin, *Drug intelligence & clinical pharmacy*. 21 (1987) 568–574. <https://doi.org/10.1177/1060028087021007-801>

M. Umamaheswari, & T. K. Chatterjee, In vitro antioxidant activities of the fractions of *Coccinia grandis* L. leaf extract, *African journal of traditional, complementary, and alternative medicines : AJTCAM*. 5 (2007) 61–73. doi:10.4314/ajtcam.v5i1.31258

V. Vilas, D. Philip, & J. Mathew, Catalytically and biologically active silver nanoparticles synthesized using essential oil, *Spectrochimica acta. Part A, Molecular and biomolecular spectroscopy*. 132 (2014) 743–750. <https://doi.org/10.1016/j.saa.2014.05.046>

R. Wahab, N. Kaushik, F. Khan, N. K. Kaushik, E. H. Choi, J. Musarrat, & A. A. Al-Khedhairi, Self-Styled ZnO Nanostructures Promotes the Cancer Cell Damage and Suppresses the Epithelial Phenotype of Glioblastoma, *Scientific reports*. 6 (2016) 19950. <https://doi.org/10.1038/srep19950>

D. Williams, The relationship between biomaterials and nanotechnology, *Biomaterials*. 29 (2008), 1737–1738. <https://doi.org/10.1016/j.biomaterials.2008.01.003>

G. Zhang, Y. Liu, X. Gao, & Y. Chen, Synthesis of silver nanoparticles and antibacterial property of silk fabrics treated by silver nanoparticles, *Nanoscale research letters*. 9 (2014) 216. <https://doi.org/10.1186/1556-276X-9-216>